Dynamics of Open-field-line MHD Experimental Configurations and Theoretical Investigation of Action Integrals as Effective Hamiltonians

P. M. Bellan[1], A. L. Moser[1], E. V. Stenson[1], R. W. Perkins[1], D. Kumar[1] and T. Shikama[1,2]

[1]Caltech, Pasadena, California, USA
[2]Kyoto University, Kyoto, Japan

Abstract:

Experiments on how Taylor relaxation actually works show that the plasma does not slowly evolve from one equilibrium state to another, but instead involves unbalanced MHD forces driving fast, localized, high density, self-collimated, magnetized plasma jets having velocity scaling proportional to electric current. The jets can undergo an instability cascade wherein a kink creates the effective gravity for a Rayleigh-Taylor instability that chokes the jet diameter to the ion skin depth at which point fast reconnection suddenly occurs. The jet internal vector magnetic field has been measured using a multi-channel optical polarimeter. An investigation into particle orbit theory shows that action integrals act as effective Hamiltonians for orbit-averaged quantities and, in particular, the various particle drifts can be found from partial derivatives of action integrals.

1 Introduction

The Caltech experimental program has the goal of determining the details underlying Taylor relaxation. Magnetized coaxial plasma guns are used to inject helicity using a topology similar to what is used in spheromaks and in tokamak DC helicity injection experiments while high speed diagnostics resolve the fastest MHD time scale. The experiments are highly reproducible. In contrast to long-pulse experiments where the configuration has repeated, random instabilities characterized as turbulence, here the pulse is short (a few μs) and the configuration evolves through a reproducible behavior. Contrary to what was expected, the plasma does not evolve through a sequence of equilibrium states as helicity is injected. Instead, the plasma is far from equilibrium, and the salient feature is highly-collimated MHD-driven plasma jets that undergo various well-defined instabilities. Typical experimental parameters are: electric current $I \sim 50 - 150$ kA, applied voltage 3-6 kV, peak plasma density $\sim 10^{21} - 10^{23}$ m^{-3}, temperature $\sim 2 - 3$ eV, jet diameter 4-8 cm, jet length up to 50 cm, jet velocity 10-50 km/s.

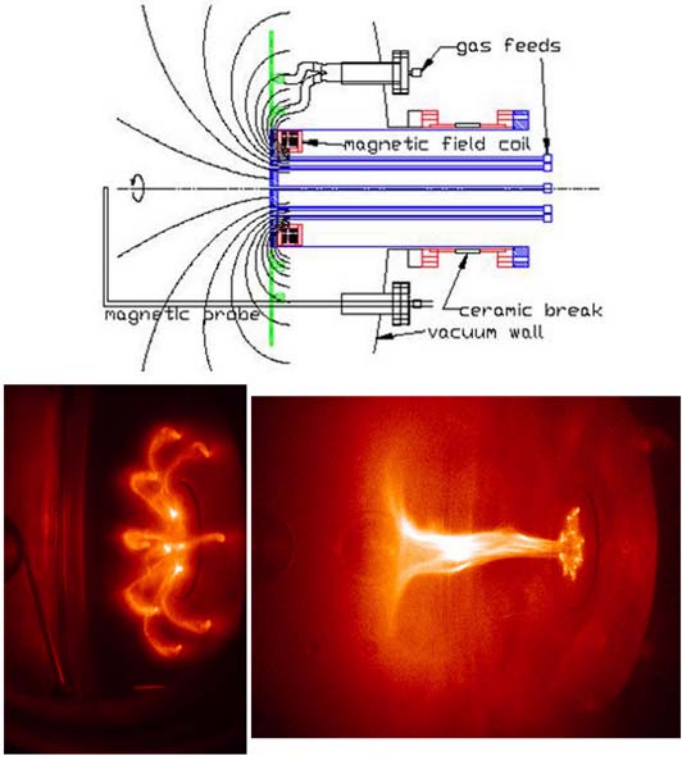

FIG. 1: Top: Layout of coaxial magnetized plasma gun. Magnetic field coil establishes poloidal bias field and then gas valves inject neutral gas from orifices in electrodes. High voltage applied between inner and outer electrodes breaks down gas to form spider legs shown in lower left. Inner segments of spider legs merge to form jet shown in lower right.

2 Jet formation and velocity measurement

Two coaxial electrodes, as shown in Fig.1, are used: a 20 cm diameter copper disk coplanar and coaxial with a copper annulus having 50 cm outside diameter. A few mm gap separates the disk from the annulus so the disk and annulus can be at different voltages. The disk and annulus each have eight gas injection orifices arranged in a circle. When a high-voltage capacitor is switched across the two electrodes, the injected gas breaks down to form eight plasma-filled arched flux tubes [1, 2]. Each arched plasma-filled flux tube spans a disk gas injection orifice and a corresponding annulus gas injection orifice. The eight flux tubes approximately follow the initial vacuum poloidal magnetic field produced by the coil resulting in a configuration reminiscent of the eight legs of a spider. Because the electric currents in the inner segments of the spider legs (i.e., near the symmetry axis) are nearly parallel and are adjacent to each other, these inner segments mutually attract and merge resulting in the formation of a central column. The central column then lengthens forming a plasma jet. The jet length increases and the jet remains highly collimated until, at a critical length, it undergoes a rapid and very distinct kink instability. The threshold for the kink is in good agreement [1, 3] with the Kruskal-Shafranov kink instability theory. Jet axial velocities are in the range of 10-50 km/s. Time-of-flight measurements [4] determined

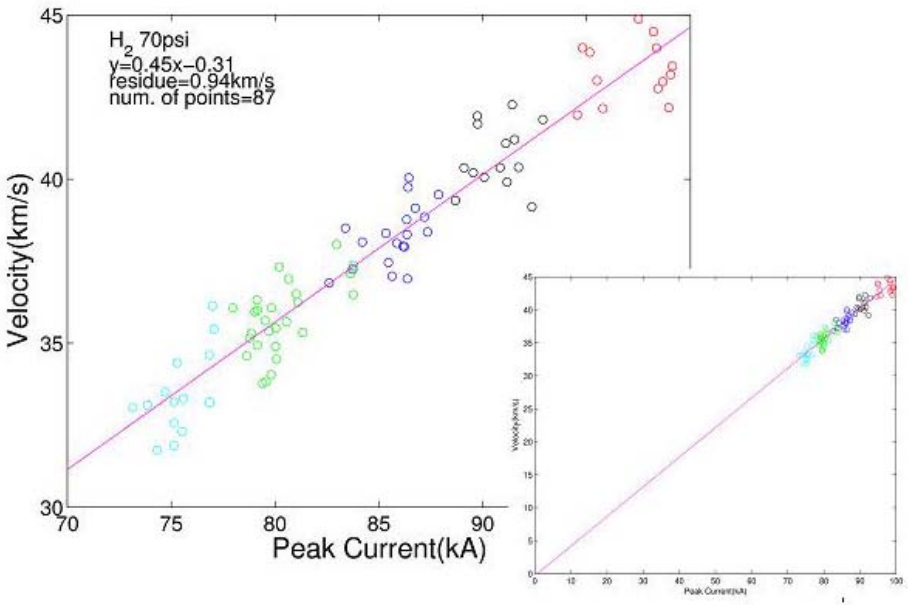

FIG. 2: Jet velocity v. gun current measured using time of flight. Inset at lower right is same data plotted with origin shown demonstrating that velocity is linearly proportional to current.

from when the jet front traverses a helium-neon laser interferometer [5] beam show in agreement with a theoretical model that the jet velocity scales as

$$U = \frac{\mu_0 I}{2\pi a\sqrt{n m_i}} \tag{1}$$

where a is the jet radius at the electrode and n is the density at the axial position where U is measured. This scaling is shown in Fig.2.

3 Kink spawning of Rayleigh-Taylor secondary instability leading to reconnection

The kink instability can spawn a Rayleigh-Taylor instability which in turn can instigate a magnetic reconnection [6]. This is "an instability of an instability", i.e., a secondary instability. Figure 3 shows the development of the kink instability during the time 20 -23 μs and then at 24 μs the sudden development of the Rayleigh-Taylor secondary instability.

More specifically, the kink instability deforms the jet into a rapidly growing helix each segment of which accelerates laterally outwards from the initial jet axis. This lateral acceleration is huge, about 10^{10} m s^{-2}. An observer in the frame of an outward accelerating jet segment would experience an effective gravity g pointing towards the initial axis. This means that there is effectively a heavy fluid (the jet segment) on 'top' of a light fluid (the low-density plasma external to the segment and closer to the initial axis). A heavy fluid

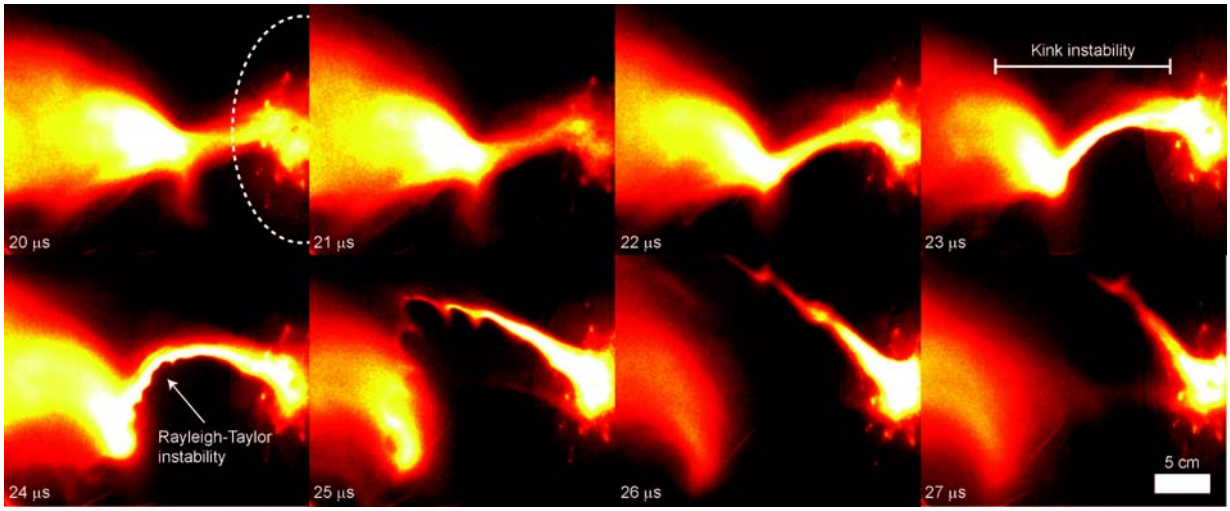

FIG. 3: Fast camera images of an argon plasma jet undergoing exponentially growing kink instability, developing a Rayleigh-Taylor instability and reconnecting [data from Moser and Bellan, Nature 482, (2012) 379].

on top of a light fluid is precisely the scenario for a Rayleigh-Taylor instability to develop. As seen in the 24 μs and 25 μs frames of Fig.3, the Rayleigh-Taylor instability consists of an inboard, axially-periodic fine structure with wavenumber k that first modulates and then quickly erodes the jet segment. The destruction of the segment effectively cuts the magnetized jet and so constitutes an explosive magnetic reconnection mechanism. The inboard location of the periodic spatial modulation (i.e., on the segment side facing the original jet axis) is consistent with the interpretation of a heavy object on a light object and the observed growth rate is in reasonable agreement with the predicted $\gamma = \sqrt{kg}$ Rayleigh-Taylor maximum theoretical growth rate (this occurs when $\mathbf{k} \cdot \mathbf{B} = 0$ where $\mathbf{k}$ is the Rayleigh-Taylor wavevector). The kink sometimes grows linearly and sometimes exponentially even though the initial conditions seem the same. The Rayleigh-Taylor instability only happens when the kink grows exponentially. This restriction makes sense because exponential kink growth provides a laterally accelerating kink segment and hence an effective gravity whereas linear kink growth gives no acceleration and hence no effective gravity. The Rayleigh-Taylor instability is seen most dramatically in nitrogen and argon plasmas where it leads to rapid erosion of the jet segment and very abrupt, essentially explosive magnetic reconnection. The Rayleigh-Taylor instability has also been observed in hydrogen plasmas but it does not erode the jet segment enough to cause magnetic reconnection. Our suspicion is that this difference is because the ion collisionless skin depth is substantially smaller in hydrogen than in nitrogen or argon. This would make it harder for the Rayleigh-Taylor instability to "choke" the current channel width down to the ion skin depth in hydrogen.

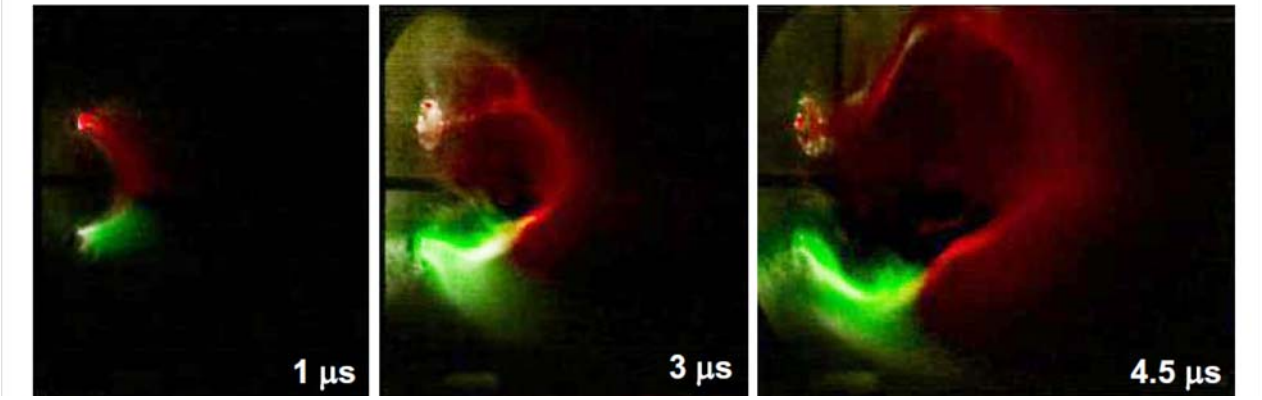

FIG. 4: Setup with hydrogen injected at top electrode and nitrogen injected at bottom electrode. MHD-driven jets originate from both electrodes. Because hydrogen jet (red) goes faster than nitrogen jet (green) the red and green jets collide closer to the bottom electrode.

4 Two opposing jets filling up a single arched magnetic flux tube

The collimation model is referred to as the "gobble" model [7] because it predicts that the MHD force effectively ingests plasma from the electrode gas orifices and then accelerates this plasma to flow as a jet into the magnetic flux tube intercepting the electrode. The jet flows from small-radius regions of the flux tube to large-radius regions because the axial force is ultimately due to the axial gradient of B_ϕ^2 where ϕ is the *local* azimuthal angle around the flux tube and z is the distance along the axis of the flux tube. Because Ampere's law gives $B_\phi = \mu_0 I/2\pi r$, B_ϕ is large near the electrode and small far from the electrode.

In another set of experiments the geometry is arranged to be analogous to a horseshoe magnet so that field lines originate at one electrode and arch over to connect to another adjacent electrode. The magnetic field is smallest at the apex of the arch since the apex is furthest from the coils producing the magnetic field. The collection of these initial vacuum field lines can be considered as an arched flux tube linking the two electrodes and this flux tube is fattest at the apex where the field is weakest so the field line density is lowest. The gobble model thus predicts that there should be axial flows from *both* cathode and anode footpoints into the flux tube so that the flux tube should fill with plasma ingested from the two footpoints. Furthermore, stagnation of the flows is predicted to cause collimation of the flux tube that almost eliminate the bulging at the apex. To test this hypothesis, a series of experiments was conducted where different gases were used at the two footpoints [8].

In a typical experiment, hydrogen was injected from the cathode electrode and nitrogen from the anode electrode, or vice versa. The plasma was then optically imaged with atomic line filters placed in front of the camera lens so as to image only the atomic line emission

of a single species. For example, an H_α filter was first used and then the experiment was repeated with a nitrogen ion atomic line filter. The images from the two identical plasma shots were then given false colors (e.g., red for hydrogen and green for nitrogen) and a composite figure was constructed showing both hydrogen and nitrogen. As shown in Fig.4 the composite figure clearly shows a red jet (hydrogen) emanating from the cathode (top) and a green jet (nitrogen) emanating from the anode (bottom) with the two jets colliding very distinctly and together filling up the flux tube with plasma. The jets lengthen, but because the hoop force causes the arch major radius to increase in the same proportion, the system increases self-similarly and the jets never intersperse. Because the hydrogen jet goes faster, the location of the jet-jet collision is not at the apex of the arch but instead is closer to the electrode from which the nitrogen jet originates. Quantitative measurements [8] support this interpretation that the arch evolves as a result of two inter-related MHD forces, namely the hoop force from the current flowing along the arch tending to increase the arch major radius and the gobble force tending to inject new plasma into the arch. Both these forces produce velocities proportional to the current flowing along the arch with the result that just enough new material enters the arch from the footpoints to keep the density of plasma in the arched flux tube constant as the flux tube lengthens.

5 Zeeman polarimeter measurement of jet magnetic field

A polarization-separating optical system has been constructed to provide temporally and spatially resolved measurements of left- and right-hand circularly polarized spectra emitted by the plasma jet. The left-and right-circularly polarized light, corresponding to Zeeman-split σ components are converted into orthogonal linearly polarized light by a wave-plate and then separated by a Glan-Thompson prism. The separated rays are then transferred by a fiber bundle to a spectrometer and the spectra from the fibers is recorded by a high-speed, gated, intensified camera. The shifts of the left- and right-hand components are proportional to the magnetic field. By using an Abel inversion technique, the radial dependence of the magnetic field is determined. Furthermore, when the jet is axisymmetric (i.e., prior to kinking) inversion of r reverses polarity of the B_ϕ component, but not the B_z component. Since the viewing line is oblique, a linear combination of B_ϕ and B_z is measured. By measuring both above and below a vertical midplane (corresponding to $+r$ and $-r$) and taking the sum and difference of the measurements, the individual contributions of B_ϕ and B_z can be separated and so the vector magnetic field is obtained. The measurements are in reasonable agreement with magnetic probe measurements and similarly indicate much larger magnetic fields in the jet than existed in the pre-jet vacuum field at the same location; this increased magnetic field is in agreement with the collimation process gathering together the original spread-out vacuum magnetic field lines frozen into the plasma.

6 Action integral as effective Hamiltonian for orbit-averaged quantities

We have shown [9] that the well-known guiding center theory particle drifts are actually a special case of a more general property of multi-dimensional Hamiltonian systems having fast oscillatory motion in one coordinate and slow changing motion in the other coordinates. The simplest example is a two-dimensional system with coordinates ξ and η where ξ undergoes a fast periodic oscillation whereas η changes only slightly during each cycle of ξ oscillation. It is shown that the change in η over a single ξ oscillation period is given by partial differentiation of the action integral J associated with ξ. This differentiation is with respect to P_η the canonical momentum conjugate to η; the quantity P_η appears as a parameter in the action integral J. This formalism retrieves the usual plasma drifts. For example, appropriate partial derivatives of $\mu = W_\perp/B$ with respect to $W_\perp$ and B retrieve the grad B drift [9]. The formalism also shows that a relativistic charged particle has a peculiar average drift velocity *parallel* to the magnetic field as a result of the mass modulation resulting from the fluctuating velocity associated with the "curlicue" $\mathbf{E} \times \mathbf{B}$ perpendicular motion. This periodic variation of the relativistic mass requires the parallel velocity to oscillate in order to keep the parallel momentum invariant. Appropriate partial derivatives of the relativistic action integral give the time-average of the oscillating parallel velocity.

More generally, the action integral is found to act as a Hamiltonian for the slow coordinate η if time is measured in units of the "tick-time" Δt of the fast oscillating coordinate ξ. Such a scaled time is obtained by defining the new "clock" time τ by

$$d\tau = dt/\Delta t \tag{2}$$

so τ advances by one unit for each period of the ξ oscillation even though the ξ period is in general not constant in time. The Hamiltonian-like equations for η, P_η are then found to be

$$\frac{d\eta}{d\tau} = \frac{\partial}{\partial P_\eta}(-J), \qquad \frac{dP_\eta}{d\tau} = -\frac{\partial}{\partial \eta}(-J) \tag{3}$$

where

$$J(\eta, P_\eta) = \oint P_\xi(\xi; \eta, P_\eta) d\xi \tag{4}$$

and η, P_η behave as slowly changing parameters in the J integral.

Acknowledgments: Supported by USDOE, NSF, AFOSR, Japan Society for the Promotion of Science

References

[1] HSU, S. C. and BELLAN, P. M. , "On the jets, kinks, and spheromaks formed by a planar magnetized coaxial gun", Physics of Plasmas 12 (2005) Art. No. 032103.

[2] YOU, S., YUN, G. S., and BELLAN, P. M., "Dynamic and stagnating plasma flow leading to magnetic-flux-tube collimation", Physical Review Letters 95 (2005) Art. 045002.

[3] HSU, S. C. and BELLAN, P. M., "A laboratory plasma experiment for studying magnetic dynamics of accretion disks and jets", Mon. Not. Royal Astron. Soc. 334 (2002) 257.

[4] KUMAR, D. and BELLAN, P. M., "Nonequilibrium Alfvenic Plasma Jets Associated with Spheromak Formation", Phys. Rev. Lett. 105 (2009) Art. No. 105003.

[5] KUMAR, D. and BELLAN, P. M., "Heterodyne interferometer with unequal path lengths", Rev. Sci. Instrum. 77 (2006) Art. No. 083503.

[6] MOSER, A. L. and BELLAN, P. M., "Magnetic reconnection from a multiscale instability cascade", Nature 482 (2012) 379.

[7] BELLAN, P. M., "Why current-carrying magnetic flux tubes gobble up plasma and become thin as a result", Phys. Plasmas 10 Pt 2 (2003) 1999.

[8] STENSON, E. V. and BELLAN, P. M., "Magnetically Driven Flows in Arched Plasma Structures", Phys. Rev. Lett. 109 (2012) Art. No. 075001.

[9] PERKINS, R. J. and BELLAN, P. M., "Wheels within Wheels: Hamiltonian Dynamics as a Hierarchy of Action Variables", Phys. Rev. Lett. 105 (2010) Art. No. 124301.